Brain Stimulation 12 (2019) 1410–1420

Contents lists available at ScienceDirect

Brain Stimulation

journal homepage: http://www.journals.elsevier.com/brain-stimulation

MR imaging central thalamic deep brain stimulation restored autistic-like social deficits in the rat

Ting-Chun Lin [a, 1], Yu-Chun Lo [b, c, 1], Hui-Ching Lin [d, 1], Ssu-Ju Li [a], Sheng-Huang Lin [e], Han-Fang Wu [d], Ming-Chia Chu [d], Chi-Wei Lee [b, d], I-Cheng Lin [f], Ching-Wen Chang [a], Yin-Chieh Liu [a], Ting-Chieh Chen [a], Yu-Ju Lin [g, **], Yen-Yu Ian Shih [h], You-Yin Chen [a, b, *]

[a] Department of Biomedical Engineering, National Yang Ming University, No.155, Sec.2, Linong St, Taipei, 11221, Taiwan, ROC
[b] The Ph.D. Program for Neural Regenerative Medicine, College of Medical Science and Technology, Taipei Medical University, No. 250 Wu-Xing St, Taipei, 11031, Taiwan, ROC
[c] Research Center for Brain and Consciousness, Taipei Medical University, Shuang Ho Hospital, No. 291, Zhongzheng Rd, New Taipei City, 23561, Taiwan, ROC
[d] Department and Institute of Physiology, National Yang Ming University, No.155, Sec.2, Linong St, Taipei, 11221, Taiwan, ROC
[e] Department of Neurology, Tzu Chi General Hospital, Tzu Chi University, No. 707, Sec. 3, Chung Yang Rd, Hualien, 97002, Taiwan, ROC
[f] Department of Psychiatry, Shuang Ho Hospital, Taipei Medical University, No. 291, Zhongzheng Rd, New Taipei City, 23561, Taiwan, ROC
[g] Department of Psychiatry, Far Eastern Memorial Hospital, No.21, Sec. 2, Nanya S. Rd, New Taipei City, 22060, Taiwan, ROC
[h] Departments of Neurology, Biomedical Engineering and Biomedical Research Imaging Center University of North Carolina at Chapel Hill, 125 Mason Farm Rd, CB# 7513, Chapel Hill, NC, 27599, USA

ARTICLE INFO

Article history:
Received 2 February 2019
Received in revised form
23 June 2019
Accepted 5 July 2019
Available online 6 July 2019

Keywords:
Autism
Central thalamic nucleus
Deep brain stimulation
Magnetic resonance imaging
Functional connectivity
Social behavior

ABSTRACT

Background: Social deficit is a core symptom in autism spectrum disorder (ASD). Although deep brain stimulation (DBS) has been proposed as a potential treatment for ASD, an ideal target nucleus is yet to be identified. DBS at the central thalamic nucleus (CTN) is known to alter corticostriatal and limbic circuits, and subsequently increase the exploratory motor behaviors, cognitive performance, and skill learning in neuropsychiatric and neurodegenerative disorders.

Objective: We first investigated the ability of CTN-DBS to selectively engage distinct brain circuits and compared the spatial distribution of evoked network activity and modulation. Second, we investigated whether CTN-DBS intervention improves social interaction in a valproic acid–exposed ASD rat offspring model.

Methods: Brain regions activated through CTN-DBS by using a magnetic resonance (MR)-compatible neural probe, which is capable of inducing site-selective microstimulations during functional MRI (fMRI), were investigated. We then performed functional connectivity MRI, the three-chamber social interaction test, and Western blotting analyses to evaluate the therapeutic efficacy of CTN-DBS in an ASD rat offspring model.

Results: The DBS-evoked fMRI results indicated that the activated brain regions were mainly located in cortical areas, limbic-related areas, and the dorsal striatum. We observed restoration of brain functional connectivity (FC) in corticostriatal and corticolimbic circuits after CTN-DBS, accompanied with increased social interaction and decreased social avoidance in the three-chamber social interaction test. The dopamine D2 receptor decreased significantly after CTN-DBS treatment, suggesting changes in synaptic plasticity and alterations in the brain circuits.

Conclusions: Applying CTN-DBS to ASD rat offspring increased FC and altered the synaptic plasticity in the corticolimbic and the corticostriatal circuits. This suggests that CTN-DBS could be an effective treatment for improving the social behaviors of individuals with ASD.

Introduction

Autism spectrum disorder (ASD) is a neurodevelopmental disorder characterized by social deficits and repetitive and

* Corresponding author. Department of Biomedical Engineering, National Yang Ming University, No.155, Sec.2, Linong St, Taipei, 11221, Taiwan, ROC.
** Corresponding author.
E-mail addresses: katrina0320@gmail.com (Y.-J. Lin), irradiance@so-net.net.tw (Y.-Y. Chen).
[1] These authors have contributed equally to this work.

https://doi.org/10.1016/j.brs.2019.07.004
1935-861X/

stereotyped behaviors [1]. Various factors, such as alterations in the brain structure or functions, genetic mutations, environmental factors including toxins, pesticides, infection, neuroinflammation, and drugs, especially exposure to valproic acid (VPA) during maternity [2], are involved in the etiopathogenesis of ASD. Studies have proven that the severity of ASD and the affected brain circuits are with high heterogeneity, which indicates that finding a specific treatment is difficult [3]. Pharmacological treatments have mainly focused on managing explicit symptoms such as irritability, aberrant social behavior, hyperactivity, repetitive behaviors, and cognitive disorders [4]. A direct and etiological pharmacological treatment that aims at addressing the fundamental problem in the brain of a person with ASD has not been established yet [5,6].

Transcranial magnetic stimulation (TMS), transcranial direct current stimulation (tDCS), and deep brain stimulation (DBS) have been proposed as alternative treatments for ASD. Repetitive TMS (rTMS) at bilateral dorsomedial prefrontal cortices has been shown to alleviate socially related impairment of ASD [7]. Individuals with ASD who received tDCS over the temporoparietal junction exhibited favorable clinical outcomes in social functioning [8]. Despite the known benefits of rTMS and tDCS in ASD, several limitations have prevented their wide applicability. The affected region can only reach the surface structures of the brain, which limits the exploration of optimal treatment targets [9]. Additionally, the spatial resolution of these modulations are limited, which increases the complexity in mechanistic precise identification of the affected cortical areas [10]. The effect duration appeared to be relatively short and symptoms usually reverted [11].

DBS has been proposed as an alternative treatment, which is a well-established neurosurgical technique that is feasible for chronic, repetitive stimulation of a defined brain area [12]. DBS alters neural activity by electrically stimulating the efferent and afferent fibers and extends modulatory effects on brain networks. Among different ASD symptoms, DBS has been demonstrated to alleviate self-injurious behavior (SIB). Bilateral globus pallidus DBS on two ASD patients reduced SIB [13]. Additionally, bilateral nucleus accumbens DBS was performed in an ASD patient with SIB, and the clinical outcome demonstrated not only a decrease in SIB but also a considerable decrease in metabolism and cortical volumes [14]. In an animal study, DBS at the subthalamic nucleus on an autism-like mouse model has been reported to inhibit repetitive stereotyped behaviors; however, the method did not inhibit social impairment [15]. The efficacy of DBS in improving social interaction deficits, one of the most prominent symptoms of ASD patients, is yet to be demonstrated. This prompted us to determine an ideal treatment target to improve social interaction through DBS.

Central thalamic nucleus (CTN) is a complex thalamic structure, which includes the central lateral (Cl), reuniens (Re), rhomboid (Rh), central medial (Cm), and parafascicular nucleus (Pf). CTN has been reported to play a key role in forebrain arousal regulation and has widespread connections with the cortex and striatum [16,17]. In clinical application, CTN-DBS has been effective in restoring consciousness of patients in coma from the vegetative state to the arousal state by regulating broad network activations, including cortical, basal ganglia, and thalamic networks [18–21]. Moreover, use of CTN-DBS on healthy nonhuman primates was reported to regulate endogenous arousal and enhance cognitive performance [22]. In a rodent study, high-frequency electrical stimulation of the CTN increased exploratory motor behaviors and enhanced cognitive performance in the novel object recognition task related to learning, memory, and preference for novelty [23]. According to our previous findings, CTN-DBS improved skill learning [24,25]. The ability of exploring novel objects, memory, and learning are essential for social interaction [26–28]. Vertes et al. demonstrated projections of CTN to the limbic-related structure, striatum, and cortex [29]; thus, CTN-DBS was likely to modulate largescale neural networks. Alteration the corticostriatal circuit [30] and limbic circuit [31] through CTN-DBS has been reported. The coricostriatal circuit has been linked to social, cognitive, and motor functions, which are known to be affected in ASD [32], and the corticolimbic circuit has been linked to the social behavior deficit [29,33].

In previous studies, DBS was demonstrated to have the ability to affect the stimulation site and distal distributed networks and promote synapse plastic circuit reorganization [34]. Dopamine has been reported to play a crucial role in regulating the synapse plastic of corticostriatal and corticolimbic circuits [35,36]. Dopamine D1 receptor (DRD1) and dopamine D2 receptor (DRD2) are two subtypes of dopamine receptors, which play contrasting roles in regulating the release of dopamine [37]. Dopamine release can promote or enhance the plasticity at corticolimbic and corticostriatal synapses [38] and alter social behaviors [39]. Moreover, several lines of evidence for the restoration of functional connectivity (FC) in brain circuits after DBS were reported [40,41]. Collectively, we hypothesized that CTN-DBS can be a potential treatment method to improve the social impairment in ASD through alteration of corticolimbic and corticostriatal circuits.

Functional MRI (fMRI) [42] and diffusion tensor imaging [43] are preferred tools for brain-wide circuit mapping studies in ASD. Although observation of the brain network through MRI has several advantages, most of the DBS electrodes are not MR-compatible, and the condition of applying MRI with DBS is restricted by the imaging distortion. Because of the severe susceptibility artifacts in DBS-MRI studies, collection of fMRI data at the stimulation site and proper interpretation of the findings is a challenge [44]. In this study, our lab-designed MR-compatible neural probes were used to perform the DBS-MRI experiment, which could reduce obstructive imaging artifacts [45–47]. To our knowledge, studies investigating the therapeutic potential of DBS applied to CTN have been limited. Therefore, we first investigated the capability of CTN-DBS to selectively engage distinct brain circuits and compared the spatial distribution of evoked network activity and modulation. Early intervention positively affected ASD symptoms in other clinical and animal studies [48,49]. In this study, the therapeutic effect of CTN-DBS on a VPA-exposed ASD model for the early-age stage, postnatal day (PND) 35, was investigated. Here, we conducted functional connectivity MRI (fcMRI) to explore the therapeutic potential of CTN-DBS applied to a VPA animal model of ASD, which delineated alterations of social-relevant circuits and demonstrated behavioral changes with circuit-targeted stimulation. Furthermore, Western blotting analysis was performed to assess the underlying mechanism of synapse plasticity alteration at the protein level.

Materials and methods

Animals

In this study, all the animals were maintained in a 12-h light-dark cycle at a room temperature of $20 \pm 3\,^{\circ}C$ and had access to food and water in the laboratory animal center of the National Yang Ming University. The experiments were performed in accordance with approved guidelines and regulations of the Institutional Animal Care and Use Committee of the National Yang Ming University.

Experiment #1: Using MRI data to validate the effect of CTN-DBS on brain regions in adult Sprague Dawley (SD) rats ($N = 5$)

Implantation surgery of neural probe in adult SD rats

Five adult male rats weighing 280–300 g were used to investigate activated brain regions induced by CTN-DBS. Two lab-designed MR-compatible neural probes (Fig. S1) were implanted

into the bilateral CTN (AP: − 3.5 mm, ML: ± 1.4 mm, DV: − 5 mm) as shown in Fig. 1A. The schematic diagram of implantation surgery was shown in Fig. 1B, and the detailed implantation surgery process was described in ***Supplemental Note 1***. Following 7-day recovery, the implanted rats were ready for evaluation of the CTN-DBS effect under fMRI.

fMRI acquisition and analysis while applying CTN-DBS in adult SD rats

fMRI acquisition and analysis of blood oxygen level dependent (BOLD) signal in response to block-design CTN-DBS paradigm. MRI was acquired using a 7-T scanner with a 30-cm diameter bore (Bruker Biospec 70/30 USR, Bruker Corp., Ettlingen, Germany), and a linear volume coil was used to transmit the radio frequency pulses. To receive the radio frequency signal, a planar surface coil (T7399V3, Bruker Corp., Billerica, MA, USA) was placed directly over the head. In the beginning of MRI experiments, each rat inhaled 3% isoflurane (Attane, Minrad Inc., Bethlehem, PA, USA) mixed with 20% O_2, 75% N_2, and 5% CO_2 for 5 min, then 0.03 mg/kg Dexdomitor was subcutaneously injected under anesthesia. Thirty minutes after the sedation, isoflurane was stopped, but the mixed air was maintained. Rats were fastened to a custom animal holder. To prevent the body temperature reduction caused by Dexdomitor [50], a heating pad, surrounding the abdomen of the rats, was adjusted to 36.5–37.5 °C. A life monitoring system and pressure sensor (SA Instruments, Inc., New York, NY, USA) were placed under the abdomen of the animals to monitor their respiratory condition. Respiration rate was maintained in the range of 45–55 breaths per minute during anatomical scans and between 65 and 75 breaths per minute during the fMRI acquiring phase.

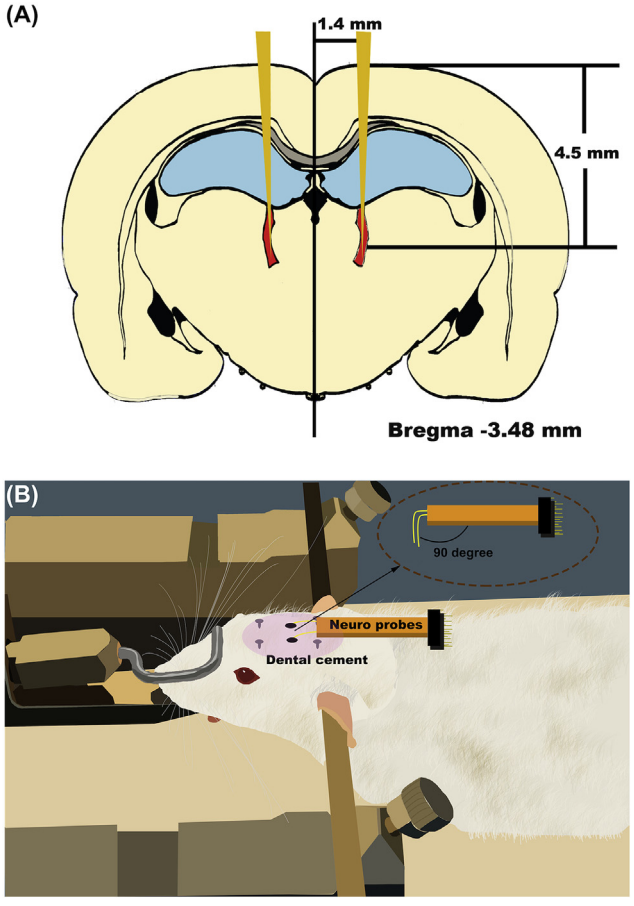

Fig. 1. (A) MR-compatible neural probes were implanted into bilateral CTN (3.5 mm posterior to the bregma, 1.4 mm lateral to the midline, and 4.5 mm ventral from the cortex surface). (B) Schematic of neural probe implantation surgery; rats were lying in the prone position on a stereotaxic device, and ear bars were fixed between their ears. Lab-designed neural probes were implanted into bilateral CTN and bended 90°, then it was fixed to the rat skull by using dental cement.

Magnetic field homogeneity was optimized using standard localized shimming with first-order shims on an isotropic voxel of $7\times 7\times 7\ mm^3$ encompassing the imaging slices. First, rapid acquisition with refocused echoes T2-weighted images were acquired (TR = 2500 ms, TE = 33 ms, matrix size = 256 × 256, field of view (FOV) = 25 × 25 mm^2, 10 coronal slices, thickness = 1 mm, number of excitations = 4), and uniform slice positioning was maintained to obtain anatomical images. Furthermore, fMRI images were acquired using gradient-echo planar imaging (GE-EPI) sequence (TR = 2000 ms, TE = 20 ms, FOV = 25 × 25 mm^2, matrix size = 80 × 80, bandwidth = 200 kHz, 10 coronal slices, and thickness = 1 mm) and CTN-DBS was performed bilaterally for five stimulation blocks and interlaced with six blocks without stimulation (block duration: 20 s). Collectively, fMRI data were collected with 10 dummy scans followed by a total of 110 vol

During stimulation, a biphasic electrical current with a pulse width of 25 μs was delivered across channels #1 and #3 on the implanted neural probe to the CTN by using an isolated stimulator (S48, Grass Technologies, West Warwick, RI, USA) with an isolated constant-current unit (PSIU6, Grass Technologies, West Warwick, RI, USA). The intensity and frequency of the electrical stimulation were 260 μA and 100 Hz, respectively.

Moreover, fMRI data was first reconstructed into 3D volume images, and then data across time were collected and reconstructed. Preprocessing analysis was performed using the FMRIB Software Library v5.0 (FSL 5.0; http://www.fmrib.ox.ac.uk/fsl) and the analysis of functional neuroimages (AFNI) software (http://afni.nimh.nih.gov/afni). The process included skull stripping, motion correction, and slice timing correction. Then, fMRI data were registered to the T2-weighted images, and linear detrending was performed to correct signal drift. Lastly, spatial smoothing with a 0.6-mm full-width half maximum (FWHM) Gaussian kernel was performed. Block design fMRI activation maps were generated using the 3dDeconvolve (general linear model function) with the given CTN-DBS stimulation paradigm. The percent BOLD signal change was calculated by normalizing data during stimulation blocks to the first nonstimulation block. To investigate the pattern among the activated brain areas, region of interests (ROIs) were selected based on clusters of functional activations. Motor cortex (M1), primary and secondary somatosensory cortices (S1 and S2 areas in SC), anterior cingulate cortex (ACC), dorsal striatum (caudate putamen, CPu), thalamus (TH), and hippocampus (Hip) were identified according to a standard brain atlas [51].

Experiment #2: fcMRI to validate the therapeutic effect of CTN-DBS on ASD model (N = 15)

Animal grouping and experimental design

To investigate the CTN-DBS therapeutic effect, rat offspring were produced and then divided into three experimental groups: (1) healthy control rat offspring ($N = 5$) with neural probes implanted but without CTN-DBS; (2) ASD DBS-OFF group ($N = 5$) with neural probes implanted in VPA-rat offspring but without CTN-DBS, and (3) ASD DBS-ON group ($N = 5$) with neural probes implanted in VPA-rat offspring and with CTN-DBS.

The experimental design and time line are depicted in Fig. 2. After a 7-day recovery period from the neural probe implantation surgery, CTN-DBS was performed on the ASD DBS-ON group for 3 days. The three-chambers test was performed on all three groups. Then, the scanned MRIs were used to investigate the FC alteration

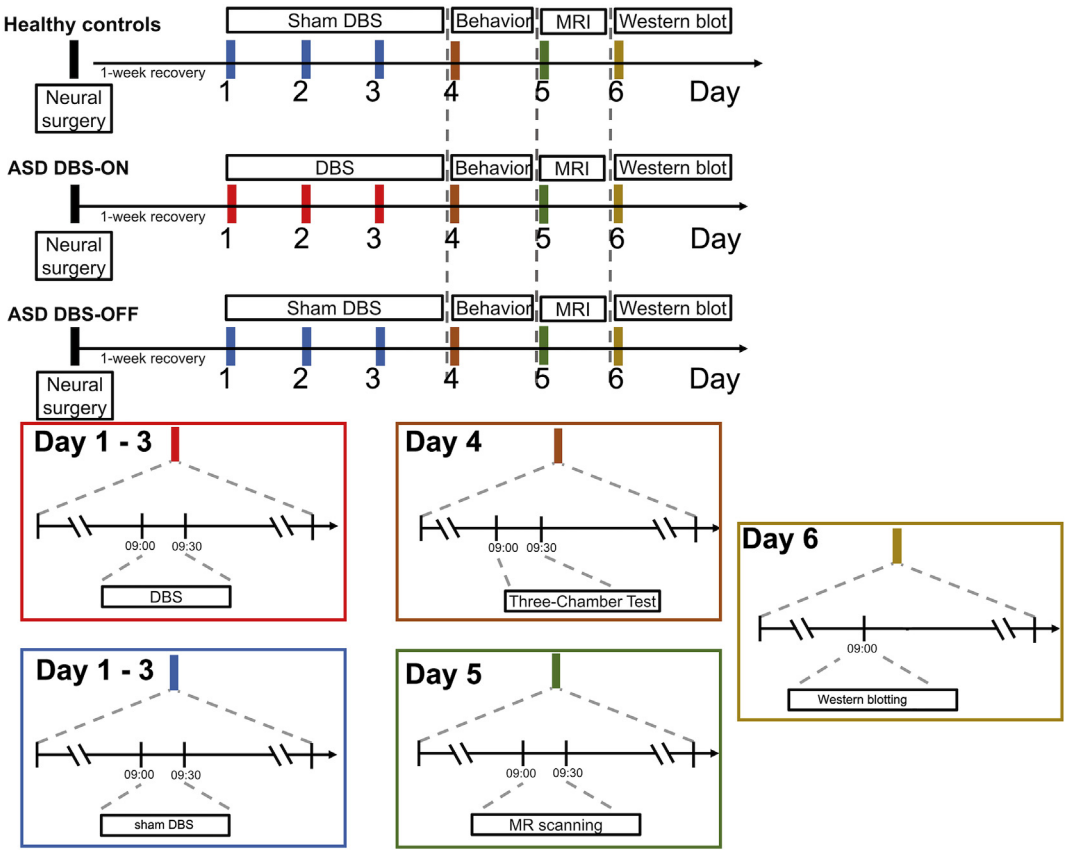

Fig. 2. Experimental protocols for CTN-DBS treatment. The rats were divided into a healthy control group, ASD DBS-ON group, and ASD DBS-OFF group. All experiments were conducted after a 1-week period of recovery from neural surgery and were followed by a daily session for the experimental procedure in all three groups. Only the ASD DBS-ON group received 30-min CTN-DBS treatment from Day 1 to Day 3. Following CTN-DBS, all animals in these three groups were sequentially subjected to a behavior test on Day 4, an MRI scan on Day 5, and Western blot analysis on Day 6. The timetable for the experiment was consistent across the groups.

after the CTN-DBS treatment. At the end of the experiments, Western blotting analysis was conducted on all rats to evaluate the dopamine receptor expression.

ASD model design

VPA is a well-known antiepileptic drug with broad applications that is commonly characterized by the mood-stabilizing properties it exhibits through regulation of gamma-aminobutyric acid (GABA) levels [52]. Several studies have suggested that VPA has a role, in combination with genetic susceptibility, in the etiology of ASD [53–56]. Because children exposed to VPA in utero demonstrate behavioral and neuroanatomical ASD features, the neuro-developmental effects of VPA were examined in rodents following prenatal or postnatal administration [57]. Studies have demonstrated that VPA exposure in rodents during embryonic development, through implantation of a single intraperitoneal VPA injection in pregnant rats, is sufficient to induce neuro-developmental and morphological features that resemble autism in humans [58–60]. These results have featured in data published on impairments in cognitive, motor, attention-related, and social development for different rodent strains, induced doses, and times of exposure. Locomotive problems were commonly observed in VPA-induced Wistar rats, and excessive self-grooming behavior was observed mostly in VPA-induced mouse strains, such as C57BL/6Hsd mice and C57BL/6 J mice [61–63]. However, in VPA-induced SD rats, the strain was associated only with sociability problems but not locomotive problems or repetitive behavior [2].

In this study, an animal model for prenatal VPA administration in SD rats was used. Adult female SD rats weighing between 280 and 300 g were used to establish an ASD-like model as were healthy control offspring from the rats' pregnancies. To produce a VPA rat model for ASD, we prepared sodium salt of valproic acid (NaVPA, Sigma-Aldrich, St. Louis, MO, USA) in 0.9% saline (100 mg/ml, pH 7.3). VPA dams at the 12th or 13th day of pregnancy received a single intraperitoneal (IP) injection of NaVPA (500 mg/kg); healthy control dams received a single injection of saline (IP, 0.9%, 3.3 ml/kg). Their male offspring were weaned on the 21st postnatal day (PND) and separated from dams.

Implantation surgery of neural probe in rat offspring

Fifteen rat offspring weighing between 180 and 200 g received the neural probe implantation surgery on PND 35 (for detailed anesthesia and surgery process, see ***Supplemental Note 1***). The neural probes were implanted into the bilateral CTN (AP: − 2.5 mm, ML: ± 1.4 mm, DV: − 4.5 mm) in the reference of the atlas of the developing rat brain [64,65] as shown in Fig. S2. Following 7-day recovery, only animals in ASD DBS-ON group were assigned to the CTN-DBS treatment.

CTN-DBS treatment

Bilateral CTN-DBS was applied to the ASD DBS-ON group in a plastic cage of diameter 30 cm and height 38 cm for 30 min once a day for 3 days. Electrical current was delivered across channel #1 (anode) to channel #3 (cathode) microelectrodes with a distance of 300 μm, which electrocuted by an isolated stimulator with an

isolated constant-current unit. The parameters of bilateral CTN-DBS were same as those described in Section 2.2.2. Although healthy controls and the ASD DBS-OFF group did not receive CTN-DBS, they were placed in the same plastic cage for 30 min. In this study, we performed a finite element method (FEM) simulation to evaluate the volume of effectively stimulated brain tissue (VTA) [45,47]. The VTA was calculated using a multicompartment cable model of a thalamocortical relay neuron [66,67]. We subsequently integrated 3D MRI and a finite element model of the neural probe to identify the intersection between the VTA and surrounding brain areas (for detailed in vivo impedance measurement and VTA results, see ***Supplemental Note 2***). Supplemental Fig. S4 shows that for channels #1 and #3, microelectrodes on the neural probe placed in the CTN produced a lower volume of VTAs than did the 3D CTN, representing a full overlap of the VTAs with the local CTN area from using our proposed stimulation parameters.

Three-chambered social interaction test

For further comparison of CTN-DBS effect on the social interaction among three rat groups, three-chambered test was used to evaluate the sociability determined by measuring the amount time the experimental rat spent approaching the chamber containing an unfamiliar rat according to Crawley's study [68]. The social interaction test was performed on each rat during the light cycle in a $60 \times 30 \times 30\,cm^3$ behavioral box divided into three chambers, namely empty, central, and social chambers, by using two fictitious lines. Each experimental rat was arranged in the central chamber for 5 min to acquire its tropism, and was then moved out of the behavioral box. A stranger rat with matching species, sex, and age to the experimental rat was randomly selected from healthy controls and was placed into the social chamber to avoid direct contact with the experimental rats. The experimental rat was placed into the behavioral box again for 5 min. Behavioral tests were recorded using a camera positioned above the behavioral box and the time spent in each chamber of each rat were analyzed by an open-source toolbox [69]. The tracking data were visualized to measure social behaviors among the healthy controls, ASD DBS-OFF group, and ASD DBS-ON group. The time spent in each chamber was recorded and calculated using the following equation:

$$Chamber\ Duration\ Rate\ (\%) = \frac{chamber\ time}{total\ time} \times 100\,\% \qquad (1)$$

where chamber time was the time that a rat spent in the empty, central, and social chambers, and the total time was the overall time a rat spent in a trial.

fcMRI acquisition and analysis

fcMRI scans were applied to each group to investigate the treatment effect of bilateral CTN-DBS. The protocol of animal anesthesia during MRI scanning and acquisition parameters were the same as that described in Section 2.2.2. The fcMRI data were acquired through 260 GE-EPI scans comprising first 10 dummy scans and 250 vol in succession. Preprocessing of fcMRI raw data was performed identically using the FSL 5.0 and AFNI software (detailed procedures also are described in Section 2.2.2) with an extra ideal band-pass filter of 0.01–0.08 Hz. GE-EPI datasets were registered to an in-house rat brain MRI template, which has which has firstly performed plane spatial smoothing (FWHM $0.6 \times 0.6\,mm^2$).

To conduct an ROI-based analysis to examine FCs between seed regions, four bilateral ROIs from the result of *experiment #1* (related to social behaviors) were chosen: M1, ACC, CPu, and Hip (Fig. S3). Seed ROIs were defined on the in-house template by using an in-house atlas, which was manually delineated based on the developing rat brain [64,65]. Cross-correlation coefficient maps between each ROI were acquired by correlating the average time course from the ROIs with the time course against whole-brain voxels. The absolute value of Pearson's correlation coefficient (r) was transformed to z-scores by using Fisher's transformation and then converted back to r values to derive group-level analysis. In this study, the normalized FC ($\widehat{FC}$) between two distinct ROIs in ASD DBS-ON or ASD DBS-OFF group compared with healthy controls at baseline was calculated using the following equation:

$$\widehat{FC}^{j}_{ROI\ A-B} = \frac{FC^{j}_{ASD\ \ ROI\ A-B}}{\frac{1}{N}\sum_{i=1}^{N} FC^{i}_{ctrl\ ROI\ A-B}} \times 100\,\% \qquad (2)$$

where the numerator of $FC^{j}_{ASD\ ROI\ A-B}$ is the j^{th} rat FC between *ROI A* and *ROI B* in ASD DBS-ON or ASD DBS-OFF group. The denominator is the mean of FC between *ROI A* and *ROI B* in healthy controls as the baseline. $FC^{i}_{ctrl\ site\ A-B}$ is the i^{th} rat FCs between *ROI A* and *ROI B*. N is the total animal numbers in healthy controls.

Western blotting analysis

To demonstrate the alteration of synaptic neurotransmitter mechanisms after CTN-DBS in the ASD rat offspring, Western blotting was used to investigate the changes in the dopaminergic system including DRD1 and the DRD2 in the striatum. The striatum was dissected from the brain tissues of the healthy controls, ASD DBS-OFF group, and ASD DBS-ON group. Protein samples were extracted in ice-cold lysis buffer (50 mM Tris-HCl, pH = 7.5, 0.3 M sucrose, 5 mM EDTA, 2 mM sodium pyrophosphate, 1 mM sodium orthovanadate, 1 mM PMSF, 20 μg/ml leupeptin, and 4 μg/ml aprotinin) and then separated (30 μg) using sodium dodecyl sulfate polyacrylamide gel electrophoresis and transferred onto polyvinylidene difluoride membranes (Millipore, Billerica, MA, USA). The membranes were hybridized with antidopamine D2 receptor (1 : 1000 dilution; ADR-002-50UL, Alomone Labs, Jerusalem, Israel) or antidopamine D1 receptor (1 : 1000 dilution; ANC-004-50UL, Alomone Labs, Jerusalem, Israel) antibodies. Next, the membranes were washed and incubated with HRP-conjugated goat antirabbit IgG antibody (1 : 1000 dilution; Jackson ImmunoResearch Inc., West Grove, PA, USA) and developed on Luminata Forte Western HRP substrate (Millipore, Billerica, MA, USA). The images were recorded using the luminescence imaging system (LAS-4000, Fujifilm, Tokyo, Japan). A gel analysis plug-in for the ImageJ software (Version 1.47, National Institutes of Health, Bethesda, MD, USA; http://imagej.nih.gov/ij/) was used to quantify the intensity of the protein bands.

Statistical analysis

In *experiment #1*, to acquire the group brain activation map induced by CTN-DBS in fMRI scans, within-group one sample t-test ($p < 0.05$; false discovery rate (FDR) < 0.05) was performed in AFNI. The percentage changes in BOLD signal variations in the DBS-ON blocks were compared with those in the DBS-OFF blocks by using the Mann-Whitney U test ($p < 0.05$).

In *experiment #2*, to acquire the group correlation map for fcMRI, within-group one sample t-test was performed in AFNI, and the significance level was set at $p < 0.05$, $FDR < 0.05$ with the minimum cluster size of 200 voxels. To compare the therapeutic effect of CTN-DBS, the $\widehat{FC}$ between ROIs was assessed using Mann-Whitney U test ($p < 0.05$) in the ASD DBS-ON and ASD DBS-OFF groups. For the social interaction comparison and protein expression level comparison, the Kruskal-Wallis test ($p < 0.05$) was performed to compare the differences among the healthy controls, ASD DBS-OFF group, and ASD DBS-ON group. A *post hoc* analysis with

Dunn's test ($p < 0.05$) was performed to evaluate the within-group difference among the healthy controls, ASD DBS-OFF group, and ASD DBS-ON group. All the aforementioned statistical analyses were performed using SPSS version 20.0 (SPSS Inc., Chicago, IL, USA), and results were presented as mean ± standard error of the mean (SEM).

Results

CTN-DBS activated brain regions

The brain areas activated by CTN-DBS were obtained from the data of five adult SD rats. Representative BOLD maps evoked by CTN-DBS are displayed in Fig. 3. Positive BOLD activations were mainly located in specific cortical areas, including M1, SC including S1 and S2, and subcortical areas, such as the CPu, ACC, and Hip ($p < 0.05$; $FDR < 0.05$, one sample t-test). The BOLD signal with CTN-DBS significantly increased in M1 with a 2.5 ± 0.03% change ($p < 0.001$), SC with 2.6 ± 0.04% change ($p < 0.001$), CPu with 3.1 ± 0.05% change ($p < 0.0001$), ACC with 2.6 ± 0.04% change ($p < 0.001$), TH with 2.8 ± 0.55% changed ($p < 0.001$) and Hip with 2.3 ± 0.07% change ($p < 0.01$).

Comparison of social interaction tests: healthy controls vs. ASD DBS-ON vs. ASD DBS-OFF

In the three-chambered social interaction test, the tracking data of the ASD DBS-ON group indicated that the rats in this group stayed longer in the stranger chamber than the rats in the ASD DBS-OFF group, suggesting that CTN-DBS improved the social behavior, as shown in Fig. 4A. The Kruskal–Wallis test revealed significant group differences among the three groups in the chamber duration rate for the empty chamber and the social chamber (empty chamber: $p = 0.039$; social chamber: $p = 0.002$). The *post hoc* analysis showed that the ASD DBS-OFF group had a significantly higher chamber duration rate in the empty chamber than the ASD DBS-ON group ($p = 0.034$) and healthy controls ($p = 0.005$), suggesting that the ASD DBS-OFF group presented social avoidance. By contrast, the ASD DBS-OFF group had a significantly lower chamber duration rate in the social chamber than the ASD DBS-ON group ($p = 0.043$) and healthy controls ($p = 0.004$), which indicated that the ASD DBS-ON group tended to explore novel objects (Fig. 4B). These results revealed that the ASD DBS-OFF group presented social impairment. However, the social interaction improved after the CTN-DBS treatment.

Comparison of FCs: healthy controls vs. ASD DBS-ON vs. ASD DBS-OFF

The CTN-DBS treatment in ASD-like rats (ASD DBS-ON group) significantly enhanced the FC between M1 and brain regions including the ACC, M1, CPu, and Hip (Fig. 5A). A significant increase in the FC of M1 with cortical area and surrounding Hip was noted. Thus, it appeared that CTN-DBS increased the FC strength in the corticostriatal circuit. A strong effect on the restoration of the FC was observed when the ACC was selected as seed after the CTN-DBS treatment (Fig. 5B). An enhanced FC was observed between the ACC and M1, Hip, and CPu, which suggested that the corticolimbic circuit was significantly enhanced after the CTN-DBS treatment. Furthermore, when Hip was selected as the seed region, the ASD DBS-OFF group appeared to exhibit considerably decreased FC, as shown in Fig. 5C. However, a significant increase in FC with CPu, M1, and ACC was observed. In Fig. 5D, when CPu was selected as the seed region, a significantly enhanced FC was found between CPu and ACC, M1, and Hip after CTN-DBS treatment.

We identified abnormal brain circuit changes between the ASD DBS-OFF group and healthy controls. The FC of corticostriatal and corticolimbic circuits in the ASD DBS-OFF group considerably

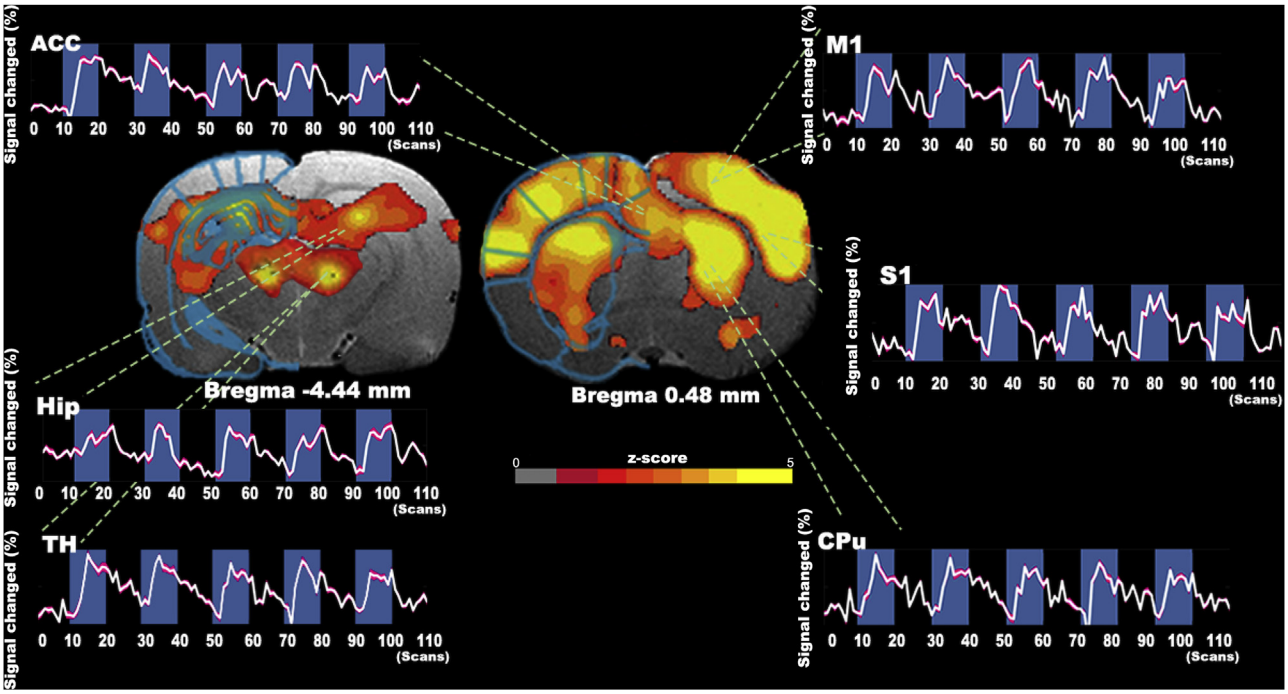

Fig. 3. Comparison of activated regions from the 220-s blocked-design paradigm with an interstimulus interval of 20-s CTN-DBS. Significant activation regions were mainly located in M1, SC (including S1 and S2), CPu, TH, ACC, and Hip (one sample t-test, $p < 0.05$, $FDR < 0.05$). Their corresponding averaged BOLD signals changed over time and were highly correlated with the blocked-design paradigm. The intervals of CTN-DBS are represented by light blue boxes with five repetitions. Data are represented as mean ± SEM. (For interpretation of the references to colour in this figure legend, the reader is referred to the Web version of this article.)

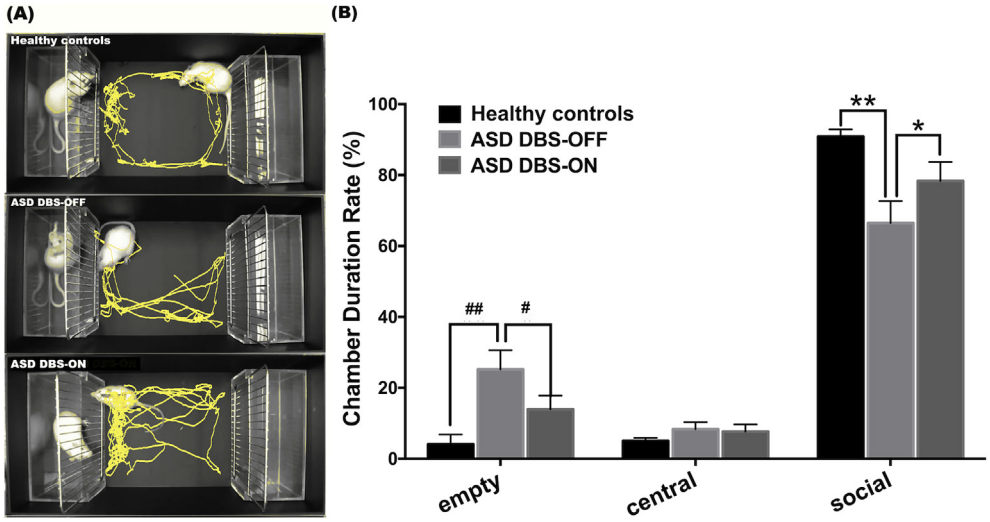

Fig. 4. (A) Overview of the three-chamber social test. The left side of the chamber is the social chamber, in which a stranger rat was randomly selected from healthy controls, and the right side is the empty chamber. Tracking trajectories are denoted by yellow lines. (B) Chamber duration rate among the healthy controls, the ASD DBS-OFF group, and the ASD DBS-ON group in the social, central, and empty chambers are plotted through bar charts. The ASD DBS-OFF group demonstrated a higher chamber duration rate than healthy controls ($p = 0.005$) and the ASD DBS-ON group ($p = 0.034$) in the empty chamber. By contrast, the ASD DBS-OFF group exhibited a lower chamber duration rate than healthy controls ($p = 0.004$) and the ASD DBS-ON group ($p = 0.043$) in the social chamber. * and ** indicate significant increases in the chamber duration rate ($p < 0.05$ and < 0.01, respectively), relative to the ASD DBS-OFF group. $^{\#}$ and $^{\#\#}$ indicate significant decreases in the chamber duration rate ($p < 0.05$ and < 0.01, respectively), relative to the ASD DBS-OFF group. All data were analyzed using the Kruskal-Wallis test and Dunn's test for post hoc analysis (mean ± SEM). (For interpretation of the references to colour in this figure legend, the reader is referred to the Web version of this article.)

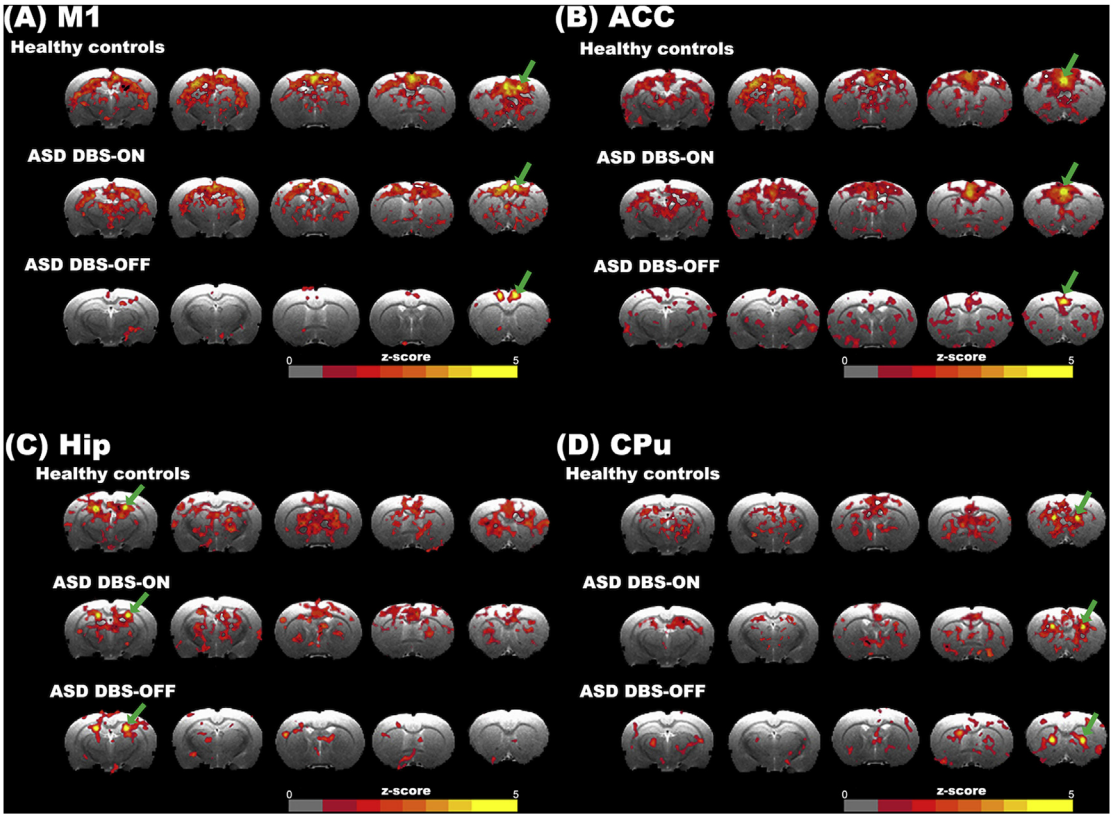

Fig. 5. Group comparisons of cross-correlation maps for healthy controls, the ASD DBS-OFF group, and the ASD DBS-ON group. The maps correspond to fcMRI for seed-ROIs placed on (A) M1, (B) ACC, (C) Hip, and (D) CPu (highlighted with green arrows in the T2-MR images). Notably, distributed but significant connectivity between various brain regions were revealed when M1, ACC, Hip, and CPu were selected as the seed regions in the healthy controls. In this study, the CTN-DBS-treated ASD group demonstrated significant restoration of FC between different brain areas with corresponding seed regions of M1, ACC, Hip, and CPu compared with the ASD DBS-OFF group. However, the ASD DBS-OFF group, by comparison, showed negligible interactions between different regions. There were highly correlated voxels within the seed region itself. Within-group one sample *t*-test was performed to acquire the FC map, and the significance level was set at $p < 0.05$ with $FDR < 0.05$ and the cluster size was corrected. . (For interpretation of the references to colour in this figure legend, the reader is referred to the Web version of this article.)

decreased, which suggested that hypoactivity in both circuits was one of the features in ASD. After the CTN-DBS treatment $\widehat{FC}_{(M1-ACC)}$ ($p = 0.032$), $\widehat{FC}_{(ACC-Hip)}$ ($p = 0.008$), $\widehat{FC}_{(M1-Hip)}$ ($p = 0.015$), $\widehat{FC}_{(M1-CPu)}$ ($p = 0.041$), $\widehat{FC}_{(ACC-CPu)}$ ($p = 0.016$), and $\widehat{FC}_{(CPu-Hip)}$ ($p = 0.008$) in the ASD DBS-ON group were significantly higher than those in the ASD DBS-OFF group, as shown in Fig. 6A. These results suggested that CTN-DBS caused the restoration of FC strength of the corticostriatal and corticolimbic circuits. Visualization of $\widehat{FC}$ in both the ASD DBS-OFF and ASD DBS-ON groups are shown in Fig. 6B.

Comparison of expression levels of the dopamine receptor: healthy controls vs. ASD DBS-ON vs. ASD DBS-OFF

The protein levels of the DRD1 and DRD2 receptors in the striatum were measured. Glyceraldehyde 3-phosphate dehydrogenase (GAPDH) was selected as the internal control with a protein weight of 34 kDa; the protein weight of the DRD1 and DRD2 receptors were 55 and 72 kDa, respectively. The protein level was normalized to GAPDH. The results of the Kruskal–Wallis test demonstrated that the DRD1 receptor exhibited no significant

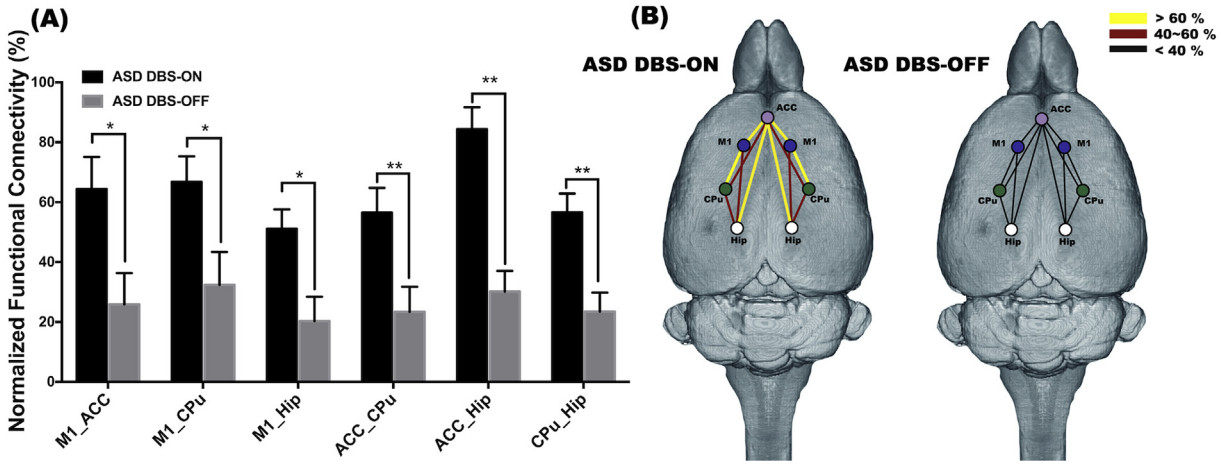

Fig. 6. (A) $\widehat{FC}$ between the selected ROIs are shown in the bar chart. The ASD DBS-OFF group indicated a widespread reduction compared with the ASD DBS-ON group after the CTN-DBS treatment. (B) $\widehat{FC}$ between the ASD DBS-ON and ASD DBS-OFF groups. Yellow lines indicate enhancement over 60%, dark red lines indicate enhancement between 40% and 60%, and black lines indicate enhancement less than 40%. *, ** and *** indicate significantly increased strength of $\widehat{FC}$ with $p < 0.05$, $p < 0.01$, and $p < 0.001$, respectively, relative to the ASD DBS-OFF group, analyzed using the Mann-Whitney *U* test (mean ± SEM). (For interpretation of the references to colour in this figure legend, the reader is referred to the Web version of this article.)

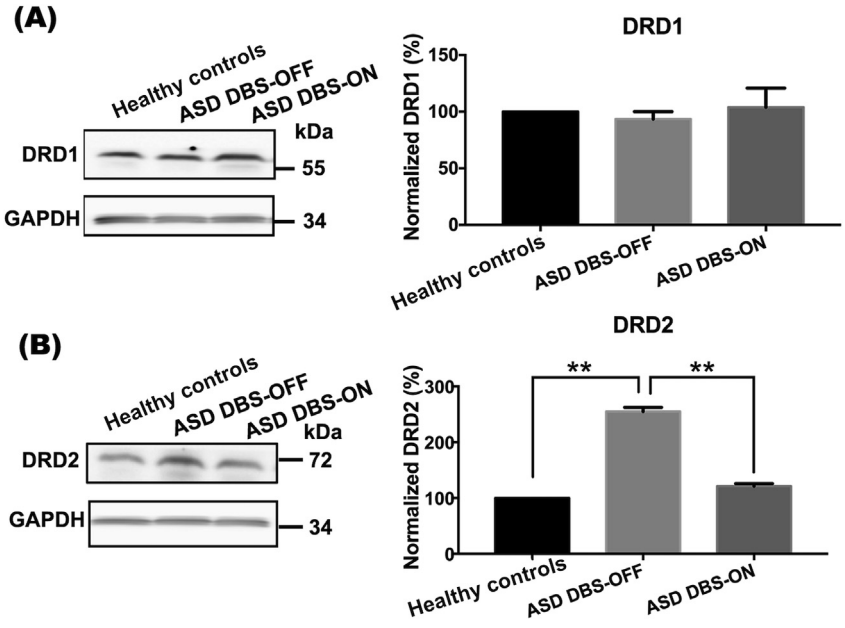

Fig. 7. Protein levels of the DRD1 and DRD2 receptors in the striatum were measured. GAPDH was selected as the internal control with a protein weight of 34 kDa; the values of the DRD1 and DRD2 receptors were 55 and 72 kDa, respectively. (A) Protein levels of DRD1 in the striatum exhibited negligible difference among healthy controls, the ASD DBS-OFF group, and the ASD DBS-ON group. (B) However, the protein level of DRD2 was significantly different between healthy controls, the ASD DBS-OFF group, and the ASD DBS-ON group ($p = 0.004$). ** indicates significant decrease in the expression level of DRD2 with $p < 0.01$, relative to the ASD DBS-OFF group, analyzed using the Kruskal-Wallis test and Dunn's test for post hoc analysis (mean ± SEM).

difference among three groups (Fig. 7A). However, the protein level of DRD2 demonstrated a significant difference among the three groups in the striatum ($p = 0.004$). The *post hoc* analysis revealed that DRD2 significantly increased within the striatum in ASD-like rats ($255 \pm 7.35\%$, $p = 0.007$) compared with in the healthy controls (Fig. 7B). After CTN-DBS treatment in ASD-like rats (ASD DBS-ON group), the striatal levels of DRD2 decreased to $121.15 \pm 4.65\%$ compared with the healthy controls. Compared with the striatal levels of DRD2 in the ASD DBS-OFF group, those in the ASD DBS-ON group were significantly lower ($p = 0.007$).

Discussion

Large scale MR imaging of brain circuit activation induced by CTN-DBS

In this study, DBS and fMRI were simultaneously used to observe in vivo network changes on a large spatial scale. We identified CTN-DBS-driven brain areas showing increased BOLD responses mainly located in cortical areas including M1, SC, and ACC, and subcortical areas including CPu, TH and Hip. Anatomical and physiological studies have demonstrated that CTN was a deep-brain relay of the forebrain to both limbic cortex and nonlimbic sites [70]. CTNs have different connections and functions; Re and Rh mainly project to the medial prefrontal cortex (PFC) and Hip, MD afferents to the PFC, Pf and Cm afferent to the PFC and motor cortex, and Cl afferents to the parietal and frontal cortex [71]. Several studies have demonstrated that Cl is connected to Cm, MD, and Rh [72–74]; once the stimulation was provided to Cl, the connected nuclei were also affected.

CTN-DBS modulated a wide variety of brain areas including M1, SC, CPu, ACC, and Hip, demonstrating that CTN is a key relay area to perform modulation on the corticostriatal and corticolimbic circuits, which were related to the social interaction regulation [75]. A human study revealed that CTN lesions led to social cognitive deficits in learning and memory, long-term information storing, problem solving, and executive functions such as verbal fluency [76]. Our study shed light on the potential target performing the global modulation of neural networks to provide a high potential therapeutic effect for social interaction in ASD.

Improvement in brain circuits and the associated social behavior in the ASD-like model through CTN-DBS modulation

Our fcMRI results indicated that the FC strength significantly decreased in the corticolimbic circuit in the ASD DBS-OFF group compared with healthy controls. Moreover, the social behavior tests in the ASD DBS-OFF group indicated apparent social avoidance and lack of exploration interest compared with healthy controls. Previous studies have discovered that an abnormal corticolimbic circuit could lead to social behavior deficit in a rodent model [33] and revealed that individuals with ASD exhibited atypical FCs in the prefrontal cortex, ACC, and Hip compared with healthy controls [77]. From fcMRI data, our study depicted that the FC strength of a corticostriatal circuit significantly decreased in the ASD DBS-OFF group compared with healthy controls. The corticostriatal circuit played a crucial role in social bonding [78], and its abnormality often indicated the changes in the functional and anatomical neural circuit associated with symptoms of ASD [32,79].

The mechanism underlying the restored-FCs in the corticostriatal circuit of the ASD-like animal model after CTN-DBS treatment may be the depolarization of striatal neurons through CTN-DBS. CTN was directly connected to the striatum and considerably affected the medium spiny striatal neurons, which have been reported to modulate the corticostriatal circuit [30]. The mechanism underlying the CTN-DBS-restored FCs in the cortico-limbic circuit may be the facilitation of long-range cortical connections due to wide point-to-point connections of the CTNs [80]. In this study, the three-chamber behavior test demonstrated improved exploration tendency and decreased latency to social behaviors after CTN-DBS treatment and enhanced FC strength in the corticostriatal and corticolimbic circuits, which indicated that CTN-DBS was an effective circuit-based intervention for ASD, especially for addressing the social behavioral problems.

Mechanisms of CTN-DBS regulation of brain circuits at the protein level

Studies have revealed that the DRD1 and DRD2 receptors, especially the DRD2 receptor, play a key role in ASD [81,82]. Hettinger et al. reported that DRD2 levels were elevated in individuals with ASD [83], and that an increase in DRD2 receptor levels could enhance the performance of the presynaptic dopamine transporter (DAT) [84] and disrupt the activity of dopamine synthesis enzyme-tyrosine hydroxylase [85], potentially resulting in the modulation of dopaminergic tone in ASD rat offspring [86,87].

In this study, we observed that the DRD2 expression level in the striatum was decreased in the ASD DBS-ON group after CTN-DBS treatment, and the ASD DBS-ON group exhibited no significant difference with healthy controls. CTN-DBS was considered to stimulate the local site and activate afferent and efferent axons [88], resulting in the release of dopamine in the terminal site, namely the striatum [89,90]. Moreover, decrease in the expression levels of DRD2 after CTN-DBS was attributed to the decrease in DAT and the increase in the dopamine synthesis enzyme [84], further increasing the synapse dopamine neurotransmission in the striatum of ASD dams [91]. Studies have confirmed that CTN-DBS balances the dysfunction of the striatal circuit in ASD [92], through increased dopamine levels [20], and increased dopamine expression in the striatum could enhance the corticostriatal circuit in ASD rat offspring [93]. This suggests that brain circuit connectivity enhancement might contribute to synaptic plasticity by altering the expression of dopaminergic receptors that modulate striatal synaptic plasticity to regulate downstream signaling cascades for improved social behavior–related brain function.

Alteration of multiple behaviors by CTN-DBS

ASD displays significant heterogeneity in its core syndrome and other behavior disturbances such as anxiety, depression, sleeping and eating disturbance attention issues, temper tantrums, and aggression or self-injury, commonly seen in autistic individuals. Several classes of pharmacological agents accounted for each ASD-related symptoms, including fluoxetine for behavioral symptoms, imipramine for antidepressants, lamotrigine for anticonvulsants and clozapine for atypical antipsychotics [94]. However, no effective medication has been established to improve the core ASD symptoms. In this study, we demonstrated that social interaction improved after CTN-DBS treatment because of the enhancement of the corticolimbic and corticostriatal circuits. Notably, the corticolimbic and corticostriatal circuits have been reported to be connected with other ASD symptoms, such as depression, anxiety, and repetitive behavior. Our study revealed that CTN-DBS increased the strength of the corticolimbic and corticalstriatal circuits, part of a wider cortico-striato-thalamo-cortical circuitry, which might decrease repetitive behaviors [95]. Collectively, CTN-DBS has a relatively broader effect in multibrain circuits, resulting in multiple behavioral improvements.

In conclusion, this study revealed that FCs in the corticolimbic and corticostriatal circuits were lower in ASD rat offspring than in

healthy controls. Applying CTN-DBS intervention to the ASD model led to higher FCs in the corticolimbic and the corticostriatal circuits, which corresponded to changes in the social interaction in ASD. Our findings suggested that CTN-DBS could be an effective treatment to improve the social behaviors in ASD.

Acknowledgements

This work is financially supported by Ministry of Science and Technology of Taiwan under Contract numbers of MOST 107-2221-E-010 -011, 107-2314-B-303 -004, 107-2221-E-035 -083 -MY2, 107-2314-B-038 -098 -MY3, 106-2314-B-038-021, 105-2314-B-038-084 and 105-2221-E-010 -014 -MY2. This work was partially supported by the NYMU-FEMH Joint Research Program (106D14). We thank 7T animal MRI Core Lab of the Neurobiology and Cognitive Science Center for technical and facility support and C. H. Hsieh and J. H. Chen of the Instrumentation Center for MRI experiments at National Taiwan University. We also take this chance to thank Dr. P.C. Chen from Department of Psychiatry at National Cheng Kung University Hospital for his kind support in consulting VPA rat model of autism.

Appendix A. Supplementary data

Supplementary data to this article can be found online at https://doi.org/10.1016/j.brs.2019.07.004.

Disclosure

All authors reported no biomedical financial interests or potential conflicts of interest.

References

[1] Lord C, Cook EH, Leventhal BL, Amaral DG. Autism spectrum disorders. Neuron 2000;28(2):355–63.
[2] Nicolini C, Fahnestock M. The valproic acid-induced rodent model of autism. Exp Neurol 2018;299:217–27.
[3] Liska A, Gomolka R, Sabbioni M, Galbusera A, Panzeri S, Scattoni ML, et al. Homozygous loss of autism-risk gene CNTNAP2 results in reduced local and long-range prefrontal functional connectivity. Cereb Cortex April 2018;28(4):1141–53.
[4] Goel R, Hong JS, Findling RL, Ji NY. An update on pharmacotherapy of autism spectrum disorder in children and adolescents. Int Rev Psychiatry 2018;30(1):78–95.
[5] LeClerc S, Easley D. Pharmacological therapies for autism spectrum disorder: a review. Pharm Therapeut 2015;40(6):389–97.
[6] Farmer C, Thurm A, Grant P. Pharmacotherapy for the core symptoms in autistic disorder: current status of the research. Drugs 2013;73(4):303–14.
[7] Enticott PG, Fitzgibbon BM, Kennedy HA, Arnold SL, Elliot D, Peachey A, et al. A double-blind, randomized trial of deep repetitive transcranial magnetic stimulation (rTMS) for autism spectrum disorder. Brain Stimul 2014;7(2):206–11.
[8] Esse Wilson J, Quinn DK, Wilson JK, Garcia CM, Tesche CD. Transcranial direct current stimulation to the right temporoparietal junction for social functioning in autism spectrum disorder: a case report. J ECT 2018;34(1):e10–3.
[9] Tremblay S, Lepage JF, Latulipe-Loiselle A, Fregni F, Pascual-Leone A, Theoret H. The uncertain outcome of prefrontal tDCS. Brain Stimul 2014;7(6):773–83.
[10] Ziemann U. TMS in cognitive neuroscience: virtual lesion and beyond. Cortex 2010;46(1):124–7.
[11] Dileone M, Mordillo-Mateos L, Oliviero A, Foffani G. Long-lasting effects of transcranial static magnetic field stimulation on motor cortex excitability. Brain Stimul 2018;11(4):676–88.
[12] Perlmutter JS, Mink JW. Deep brain stimulation. Annu Rev Neurosci 2006;29:229–57.
[13] Stocco A, Baizabal-Carvallo JF. Deep brain stimulation for severe secondary stereotypies. Park Relat Disord 2014;20(9):1035–6.
[14] Park HR, Kim IH, Kang H, Lee DS, Kim BN, Kim DG, et al. Nucleus accumbens deep brain stimulation for a patient with self-injurious behavior and autism spectrum disorder: functional and structural changes of the brain: report of a case and review of literature. Acta Neurochir 2017;159(1):137–43.
[15] Chang AD, Berges VA, Chung SJ, Fridman GY, Baraban JM, Reti IM. High-frequency stimulation at the subthalamic nucleus suppresses excessive self-grooming in autism-like mouse models. Neuropsychopharmacology : Off Publ Am Coll Neuropsychopharmacol 2016;41(7):1813–21.
[16] Jones EG. Synchrony in the interconnected circuitry of the thalamus and cerebral cortex. Ann N Y Acad Sci 2009;1157:10–23.
[17] Schiff ND, Giacino JT, Kalmar K, Victor JD, Baker K, Gerber M, et al. Behavioural improvements with thalamic stimulation after severe traumatic brain injury. Nature 2007;448(7153):600–3.
[18] Schiff ND, Fins JJ. Brain death and disorders of consciousness. Curr Biol 2016;26(13):R572–6.
[19] Liu J, Lee HJ, Weitz AJ, Fang Z, Lin P, Choy M, et al. Frequency-selective control of cortical and subcortical networks by central thalamus. Elife 2015;4:e09215.
[20] Schiff ND. Central thalamic deep brain stimulation for support of forebrain arousal regulation in the minimally conscious state. Handb Clin Neurol 2013;116:295–306.
[21] Kundishora AJ, Gummadavelli A, Ma C, Liu M, McCafferty C, Schiff ND, et al. Restoring conscious arousal during focal limbic seizures with deep brain stimulation. Cereb Cortex 2017;27(3):1964–75.
[22] Baker JL, Ryou J-W, Wei XF, Butson CR, Schiff ND, Purpura KP. Robust modulation of arousal regulation, performance, and frontostriatal activity through central thalamic deep brain stimulation in healthy nonhuman primates. J Neurophysiol 2016;116(5):2383–404.
[23] Shirvalkar P, Seth M, Schiff ND, Herrera DG. Cognitive enhancement with central thalamic electrical stimulation. Proc Natl Acad Sci U S A 2006;103(45):17007–12.
[24] Lin HC, Pan HC, Lin SH, Lo YC, Shen ET, Liao LD, et al. Central thalamic deep-brain stimulation alters striatal-thalamic connectivity in cognitive neural behavior. Front Neural Circuits 2015;9:87.
[25] Wang CF, Yang SH, Lin SH, Chen PC, Lo YC, Pan HC, et al. A proof-of-principle simulation for closed-loop control based on preexisting experimental thalamic DBS-enhanced instrumental learning. Brain Stimul 2017;10(3):672–83.
[26] Adaval R, Wyer RS. Communicating about a social interaction: effects on memory for protagonists' statements and nonverbal behaviors. J Exp Soc Psychol 2004;40(4):450–65.
[27] Kaidanovich-Beilin O, Lipina T, Vukobradovic I, Roder J, Woodgett JR. Assessment of social interaction behaviors. J Vis Exp : J Vis Exp 2011;(48):2473.
[28] Okita SY. Social interactions and learning. In: Seel NM, editor. Encyclopedia of the sciences of learning. Boston, MA: Springer US; 2012. p. 3104–7.
[29] Vertes RP, Linley SB, Hoover WB. Limbic circuitry of the midline thalamus. Neurosci Biobehav Rev 2015;54:89–107.
[30] Shah SA, Schiff ND. Central thalamic deep brain stimulation for cognitive neuromodulation–a review of proposed mechanisms and investigational studies. Eur J Neurosci 2010;32(7):1135–44.
[31] Kim JP, Min H-K, Knight EJ, Duffy PS, Abulseoud OA, Marsh MP, et al. Centromedian-parafascicular deep brain stimulation induces differential functional inhibition of the motor, associative, and limbic circuits in large animals. Biol Psychiatry 2013;74(12):917–26.
[32] Balsters JH, Mantini D, Wenderoth N. Connectivity-based parcellation reveals distinct cortico-striatal connectivity fingerprints in Autism Spectrum Disorder. Neuroimage 2018;170:412–23.
[33] Rincón-Cortés M, Sullivan RM. Emergence of social behavior deficit, blunted corticolimbic activity and adult depression-like behavior in a rodent model of maternal maltreatment. Transl Psychiatry 2016;6:e930.
[34] Veerakumar A, Berton O. Cellular mechanisms of deep brain stimulation: activity-dependent focal circuit reprogramming? Curr Opin Behav Sci 2015;4:48–55.
[35] Haber SN. Corticostriatal circuitry. Dialogues Clin Neurosci 2016;18(1):7–21.
[36] Adams B, Moghaddam B. Corticolimbic dopamine neurotransmission is temporally dissociated from the cognitive and locomotor effects of phencyclidine. J Neurosci : Off J Soc Neurosci 1998;18(14):5545–54.
[37] Eagle DM, Wong JCK, Allan ME, Mar AC, Theobald DE, Robbins TW. Contrasting roles for dopamine D1 and D2 receptor subtypes in the dorsomedial striatum but not the nucleus accumbens core during behavioral inhibition in the stop-signal task in rats. J Neurosci 2011;31(20):7349.
[38] Shiflett MW, Balleine BW. Contributions of ERK signaling in the striatum to instrumental learning and performance. Behav Brain Res 2011;218(1):240–7.
[39] Torquet N, Marti F, Campart C, Tolu S, Nguyen C, Oberto V, et al. Social interactions impact on the dopaminergic system and drive individuality. Nat Commun 2018;9(1):3081.
[40] Figee M, Luigjes J, Smolders R, Valencia-Alfonso CE, van Wingen G, de Kwaasteniet B, et al. Deep brain stimulation restores frontostriatal network activity in obsessive-compulsive disorder. Nat Neurosci 2013;16(4):386–7.
[41] Schweder PM, Joint C, Hansen PC, Green AL, Quaghebeur G, Aziz TZ. Chronic pedunculopontine nucleus stimulation restores functional connectivity. Neuroreport 2010;21(17):1065–8.
[42] Dichter GS. Functional magnetic resonance imaging of autism spectrum disorders. Dialogues Clin Neurosci 2012;14(3):319–51.
[43] Mori S, Zhang J. Principles of diffusion tensor imaging and its applications to basic neuroscience research. Neuron 2006;51(5):527–39.
[44] Balachandran R, Welch EB, Dawant BM, Fitzpatrick JM. Effect of MR distortion on targeting for deep-brain stimulation. IEEE Trans Biomed Eng 2010;57(7):1729–35.
[45] Chen YY, Lai HY, Lin SH, Cho CW, Chao WH, Liao CH, et al. Design and fabrication of a polyimide-based microelectrode array: application in neural

recording and repeatable electrolytic lesion in rat brain. J Neurosci Methods 2009;182(1):6–16.
[46] Yang PF, Chen YY, Chen DY, Hu JW, Chen JH, Yen CT. Comparison of fMRI BOLD response patterns by electrical stimulation of the ventroposterior complex and medial thalamus of the rat. PLoS One 2013;8(6):e66821.
[47] Lai H-Y, Younce JR, Albaugh DL, Kao Y-CJ, Shih Y-YI. Functional MRI reveals frequency-dependent responses during deep brain stimulation at the subthalamic nucleus or internal globus pallidus. Neuroimage 2014;84:11–8.
[48] Landa RJ. Efficacy of early interventions for infants and young children with, and at risk for, autism spectrum disorders. Int Rev Psychiatry 2018;30(1):25–39.
[49] Dai Y-C, Zhang H-F, Schön M, Böckers TM, Han S-P, Han J-S, et al. Neonatal oxytocin treatment ameliorates autistic-like behaviors and oxytocin deficiency in valproic acid-induced rat model of autism. Front Cell Neurosci 2018;12:355.
[50] Hopfensperger MJ, Messenger KM, Papich MG, Sherman BL. The use of oral transmucosal detomidine hydrochloride gel to facilitate handling in dogs. J Vet Behav Clin Appl Res 2013;8(3):114–23.
[51] Paxinos G, Watson C. The rat brain in stereotaxic coordinates. Academic Press; 2007.
[52] Moeller JJ, Rahey SR, Sadler RM. Lamotrigine–valproic acid combination therapy for medically refractory epilepsy. Epilepsia 2009;50(3):475–9.
[53] Bromley R, Mawer G, Clayton-Smith J, Baker G, Liverpool, Group MN. Autism spectrum disorders following in utero exposure to antiepileptic drugs. Neurology 2008;71(23):1923–4.
[54] Williams G, King J, Cunningham M, Stephan M, Kerr B, Hersh JH. Fetal valproate syndrome and autism: additional evidence of an association. Dev Med Child Neurol 2001;43(03):202–6.
[55] Kazdoba TM, Leach PT, Yang M, Silverman JL, Solomon M, Crawley JN. Translational mouse models of autism: advancing toward pharmacological therapeutics. Curr Top Behav Neurosci 2016;28:1–52.
[56] Crawley JN. Translational animal models of autism and neurodevelopmental disorders. Dialogues Clin Neurosci 2012;14(3):293–305.
[57] Wagner GC, Reuhl KR, Cheh M, McRae P, Halladay AK. A new neurobehavioral model of autism in mice: pre- and postnatal exposure to sodium valproate. J Autism Dev Disord 2006;36(6):779–93.
[58] Roullet FI, Lai JK, Foster JA. In utero exposure to valproic acid and autism–a current review of clinical and animal studies. Neurotoxicol Teratol 2013;36:47–56.
[59] Chapman JB, Cutler MG. Sodium valproate: effects on social behaviour and physical development in the mouse. Psychopharmacology (Berl) 1984;83(4):390–6.
[60] Schneider T, Przewlocki R. Behavioral alterations in rats prenatally exposed to valproic acid: animal model of autism. Neuropsychopharmacology : Off Publ Am Coll Neuropsychopharmacol 2005;30(1):80–9.
[61] Markram K, Rinaldi T, La Mendola D, Sandi C, Markram H. Abnormal fear conditioning and amygdala processing in an animal model of autism. Neuropsychopharmacology : Off Publ Am Coll Neuropsychopharmacol 2008;33(4):901–12.
[62] Rinaldi T, Perrodin C, Markram H. Hyper-connectivity and hyper-plasticity in the medial prefrontal cortex in the valproic Acid animal model of autism. Front Neural Circuits 2008;2:4.
[63] Al-Askar M, Bhat RS, Selim M, Al-Ayadhi L, El-Ansary A. Postnatal treatment using curcumin supplements to amend the damage in VPA-induced rodent models of autism. BMC Complement Altern Med 2017;17(1):259.
[64] Sherwood NM, Timiras PS. A stereotaxic atlas of the developing rat brain. University of California Press; 1970.
[65] Calabrese E, Badea A, Watson C, Johnson GA. A quantitative magnetic resonance histology atlas of postnatal rat brain development with regional estimates of growth and variability. Neuroimage 2013;71:196–206.
[66] McIntyre CC, Grill WM, Sherman DL, Thakor NV. Cellular effects of deep brain stimulation: model-based analysis of activation and inhibition. J Neurophysiol 2004;91(4):1457–69.
[67] Kent AR, Swan BD, Brocker DT, Turner DA, Gross RE, Grill WM. Measurement of evoked potentials during thalamic deep brain stimulation. Brain Stimul 2015;8(1):42–56.
[68] Crawley JN. Designing mouse behavioral tasks relevant to autistic-like behaviors. Ment Retard Dev Disabil Res Rev 2004;10(4):248–58.
[69] Patel TP, Gullotti DM, Hernandez P, O'Brien WT, Capehart BP, Morrison B, et al. An open-source toolbox for automated phenotyping of mice in behavioral tasks. Front Behav Neurosci 2014;8(349).
[70] Hoover WB, Vertes RP. Collateral projections from nucleus reuniens of thalamus to hippocampus and medial prefrontal cortex in the rat: a single and double retrograde fluorescent labeling study. Brain Struct Funct 2012;217(2):191–209.
[71] Saalmann YB. Intralaminar and medial thalamic influence on cortical synchrony, information transmission and cognition. Front Syst Neurosci 2014;8(83).
[72] Mengual E, de las Heras S, Erro E, Lanciego JL, Giménez-Amaya JM. Thalamic interaction between the input and the output systems of the basal ganglia. J Chem Neuroanat 1999;16(3):187–200.
[73] Deschênes M, Bourassa J, Parent A. Striatal and cortical projections of single neurons from the central lateral thalamic nucleus in the rat. Neuroscience 1996;72(3):679–87.
[74] Yurgelun-Todd DA, Rogowska J, Gruber SA, Bogorodzki P, Simpson NS, Irvin RW, et al. Increased amygdala fMRI activation after secretin administration. Exp Clin Psychopharmacol 2008;16(3):191–8.
[75] Schiff ND. Central thalamic contributions to arousal regulation and neurological disorders of consciousness. Ann N Y Acad Sci 2008;1129(1):105–18.
[76] Wilkos E, Brown TJ, Slawinska K, Kucharska KA. Social cognitive and neurocognitive deficits in inpatients with unilateral thalamic lesions - pilot study. Neuropsychiatric Dis Treat 2015;11:1031–8.
[77] Solomon M, Ragland JD, Niendam TA, Lesh TA, Beck JS, Matter JC, et al. Atypical learning in autism spectrum disorders: a functional magnetic resonance imaging study of transitive inference. J Am Acad Child Adolesc Psychiatry 2015;54(11):947–55.
[78] Amadei EA, Johnson ZV, Jun Kwon Y, Shpiner AC, Saravanan V, Mays WD, et al. Dynamic corticostriatal activity biases social bonding in monogamous female prairie voles. Nature 2017;546(7657):297–301.
[79] Fuccillo MV. Striatal circuits as a common node for autism pathophysiology. Front Neurosci 2016;10:27.
[80] Schiff ND. Central thalamic deep-brain stimulation in the severely injured brain: rationale and proposed mechanisms of action. Ann N Y Acad Sci 2009;1157:101–16.
[81] Martinez D, Orlowska D, Narendran R, Slifstein M, Liu F, Kumar D, et al. Dopamine type 2/3 receptor availability in the striatum and social status in human volunteers. Biol Psychiatry 2010;67(3):275–8.
[82] Yamaguchi Y, Lee YA, Kato A, Jas E, Goto Y. The roles of dopamine D2 receptor in the social hierarchy of rodents and primates. Sci Rep 2017;7:43348.
[83] Hettinger JA, Liu X, Hudson ML, Lee A, Cohen IL, Michaelis RC, et al. DRD2 and PPP1R1B (DARPP-32) polymorphisms independently confer increased risk for autism spectrum disorders and additively predict affected status in male-only affected sib-pair families. Behav Brain Funct 2012;8:19.
[84] Lee FJ, Pei L, Moszczynska A, Vukusic B, Fletcher PJ, Liu F. Dopamine transporter cell surface localization facilitated by a direct interaction with the dopamine D2 receptor. EMBO J 2007;26(8):2127–36.
[85] Lindgren N, Xu ZQ, Herrera-Marschitz M, Haycock J, Hokfelt T, Fisone G. Dopamine D(2) receptors regulate tyrosine hydroxylase activity and phosphorylation at Ser40 in rat striatum. Eur J Neurosci 2001;13(4):773–80.
[86] Floresco SB, Magyar O, Ghods-Sharifi S, Vexelman C, Tse MT. Multiple dopamine receptor subtypes in the medial prefrontal cortex of the rat regulate set-shifting. Neuropsychopharmacology : Off Publ Am Coll Neuropsychopharmacol 2006;31(2):297–309.
[87] Squillace M, Dodero L, Federici M, Migliarini S, Errico F, Napolitano F, et al. Dysfunctional dopaminergic neurotransmission in asocial BTBR mice. Transl Psychiatry 2014;4:e427.
[88] McCracken CB, Kiss ZH. Time and frequency-dependent modulation of local field potential synchronization by deep brain stimulation. PLoS One 2014;9(7):e102576.
[89] McIntyre CC, Anderson RW. Deep brain stimulation mechanisms: the control of network activity via neurochemistry modulation. J Neurochem 2016;139:338–45.
[90] Varela C. Thalamic neuromodulation and its implications for executive networks. Front Neural Circuits 2014;8:69.
[91] Lee SA, Suh Y, Lee S, Jeong J, Kim SJ, Kim SJ, et al. Functional expression of dopamine D2 receptor is regulated by tetraspanin 7-mediated postendocytic trafficking. FASEB J : Off Publ Fed Am Soc Exp Biol 2017;31(6):2301–13.
[92] Di Martino A, Kelly C, Grzadzinski R, Zuo XN, Mennes M, Mairena MA, et al. Aberrant striatal functional connectivity in children with autism. Biol Psychiatry 2011;69(9):847–56.
[93] Kayser AS, Allen DC, Navarro-Cebrian A, Mitchell JM, Fields HL. Dopamine, corticostriatal connectivity, and intertemporal choice. J Neurosci 2012;32(27):9402.
[94] Kumar B, Prakash A, Sewal RK, Medhi B, Modi M. Drug therapy in autism: a present and future perspective. Pharmacol Rep : PR 2012;64(6):1291–304.
[95] Li B, Mody M. Cortico-striato-thalamo-cortical circuitry, working memory, and obsessive–compulsive disorder. Front Psychiatry 2016;7:78.